Effects of the Interaction between Intercalant and Matrix Polymer in Preparation of Clay-dispersed Nanocomposite

Moon Bae Ko*, Jyunkyung Kim, and Chul Rim Choe

Polymer Hybrid Research Center, Korea Institute of Science and Technology, Seoul 130-650, Korea

Abstract : Clay-dispersed nanocomposites have been prepared by simple melt-mixing of two components, styrenic polymers with different content of functional groups and two different organophilic clays (Cloisite$^\circledR$ 25A and Cloisite$^\circledR$ 30A) with a twin screw extruder. Dispersibility of 10-Å-thick silicate layers of clay in the hybrid was investigated by using an X-ray diffraction method and a transmission electron microscope. It was found that if the interaction force between intercalant and matrix polymer is attractive, the matrix polymer intercalates more rapidly into the gallery of silicate layers. The faster intercalation of matrix polymer leads to the better dispersibility of silicate layers in the matrix polymer.

Introduction

Dispersion of smectite clays and other layered inorganic materials that can be broken down into nano-scale building blocks in the polymer matrix is a good method for the preparation of organic-inorganic nanocomposites. While nanocomposites can be made in a number of ways, this paper will report on studies of melt blending the clay into the polymer. The inorganic MMT surface is modified by organic treatments to make the platelet more compatible with the organic polymer. It is well documented that the choice of organic treatment influences the degree of dispersion of the MMT in the polymer matrix.[1-7] This paper will shows that the selection of intercalant for a matrix polymer can significantly influence the degree of dispersion in the melt blending process. In present work, clay/polymer hybrids have been prepared by simple melt-mixing of two components with a twin screw extruder. Two different matrix polymer, i.e. poly(styrene-co-acrylonitrile) copolymer (SAN) and poly(styrene-co-methylvinyloxazoline) copolymer (oxaPS) were used in order to compare the effects of the content of functional group on the intercalation-

and exfoliation-behavior of the organophilic clays. Also, two different organophilic clays were used in order to compare the effect of the interaction between intercalant and matrix polymer on the intercalation- and exfoliation-behavior of the organophilic clays. Dispersibility of 10-Å-thick silicate layers in the hybrids was investigated by using a transmission electron microscope and an X-ray diffraction method.

Experimental

Materials. "Cloisite$^\circledR$" supplied by Southern Clay Products Inc. is trade name of organophilic clays. Two kinds of intercalants were used in the study: dimethyl hydrogenated-tallow (2-ethylhexyl) ammonium (2MHTL8), and methyl tallow bis-2hydroxyethyl ammonium (MT-2EthOH). It is note-worthy that a molecule of MT-2EthOH has two hydroxyl groups, thus the intercalant can have the specific interaction with the polymers with functional groups, i.e. nitrile group, methylvinyloxazoline group, etc. Chemical structures of intercalants are depicted in Figure 1, where HT is predominantly an octadecyl chain with smaller amounts of lower homologues (approximate composition: 65% C18, 30% C16, 5% C14). Its inorganic content was cal-

---

*e-mail : mbko@kistmail.kist.re.kr

Table I. Charateristic Properties of the Organophilic Clays Used in the Study

Code	Organic Modifier	Modifier Concentration (meq/100 g)	Weight Loss on Ignition(%)	d-spacing (Å)
C25A	2MHTL8	95	34	20.0
C30A	MT-2EthOH	95	32	18.2
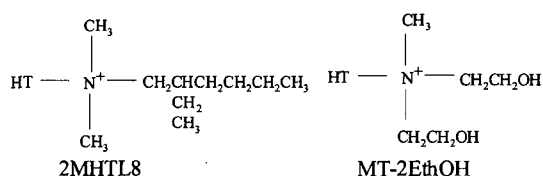
Figure 1. Chemical structure of intercalants used in the study.
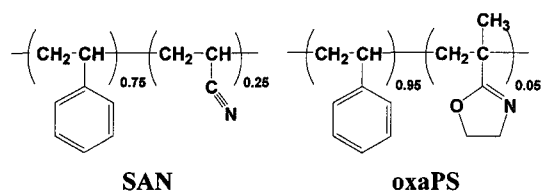
Figure 2. Chemical structures of two copolymers used in the study.

culated by measuring the weights before and after burning its organic parts. The basal spacing of organophilic clay was measured by an X-ray diffraction method. The characteristic properties of organophilic clays are summarized in Table I. Poly(styrene-co-acrylonitrile) copolymer (M_w= 107,000, AN content=25 wt%) was obtained from Cheil Industries Inc. and poly(styrene-co-methyl-vinyloxazoline) copolymer (M_w=188,000, MVOZ content=5 wt%) was supplied from Nippon Shokubai. The chemical structures of two copolymers used in the study are depicted in Figure 2. They were used after dried in a vacuum oven at 80 °C for more than 24 hours.

Preparation of Hybrids. Powdery two components of organophilic clay and matrix polymer were dry-mixed. The mixture was melt-blended by using a twin screw extruder (Model TSE 16TC, Prism) at 180°C to yield pale-yellow strand of the hybrids. The obtained strands were chopped with a pelletizer. In order to prepare the samples having different degrees of clay-dispersion, the hybrid pellets were multi-processed in a twin screw extruder up to five extrusion-cycles. For this study

the inorganic content in the hybrids was fixed at 5 wt%.

Evaluation of the Dispersibility of Clay. Dispersibility of silicates layers in the hybrids was evaluated by using an X-ray diffractometer and a transmission electron micrograph (TEM). An X-ray diffractometer (Model MXP18, MacScience) was adopted to monitor the change in d-spacing of montmorillonite before and after intercalation. CuK_α(=1.54 Å) was used as X-ray source at a generator voltage of 40 kV and current of 100 mA. The scanning rate was 0.2 °/min. The basal spacing of the silicate layers, d, was calculated using the Bragg's law, $\lambda=2d\sin\theta$ from the position of the (001) plane peak in XRD pattern. TEM (Model CN30, Philips) observations of the hybrids were performed for the injection-molded samples, and were operated at an acceleration voltage of 120 kV. Thin sections of 70 nm were microtomed with a diamond knife and then subjected to TEM observation without staining.

Results and Discussion

Figure 3 shows the temporal series of XRD patterns from the C25A/SAN-, C30A/SAN-, C25A/oxaPS-, C30A/oxaPS-hybrids melt-mixed with the twin screw extruder. Each XRD pattern in the figure was shifted to the appropriate intensity in the upward direction in order to make each curve preventing from overlapping of each other. Figure 3(a) and (b) show the XRD patterns from C25A/SAN- and C30A/SAN-hybrids, respectively. The d-spacings calculated from the peak position in XRD patterns of C30A/SAN-hybrids are greater than those of C25A/SAN-hybrids. Also, it is distinct that the peak intensities for the C30A/SAN-hybrids are weaker than those for C25A/SAN-hybrids, which indicates that much more silicate layers in the C30A/SAN-hybrids were exfoliated than those for C25A/SAN-hybrids. It can be found that while the peak in the XRD patterns
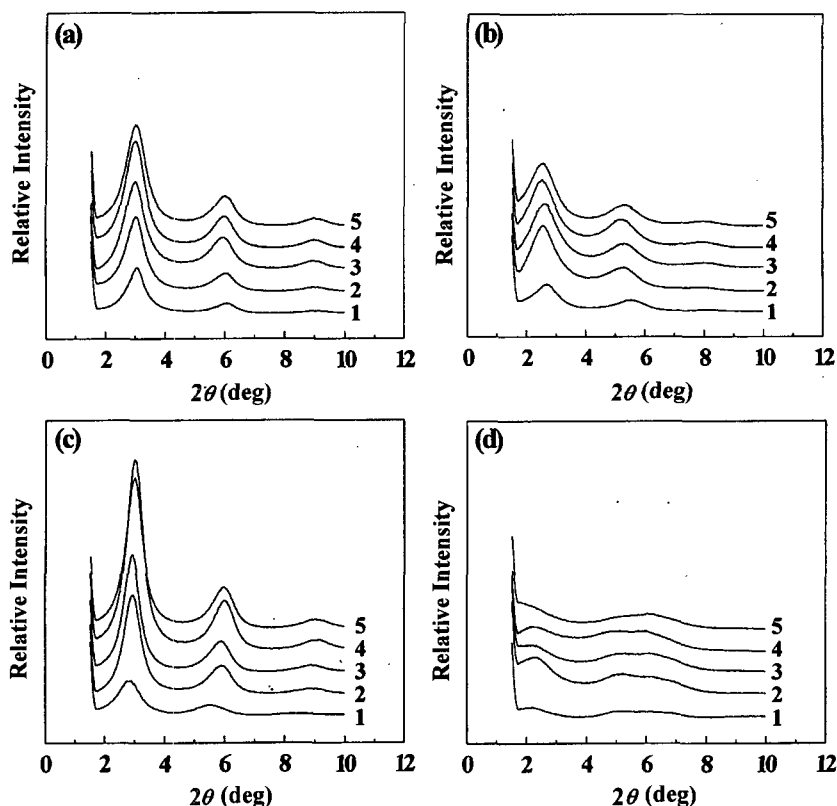
Figure 3. Temporal series of XRD patterns from the (a) C25A/SAN-, (b) C30A/SAN-, (c) C25A/oxaPS-, and (d) C30A/ oxaPS-hybrid, respectively. The numbers in the figure indicate the extrusion-cycle.

from C25A/oxaPS-hybrid (Figure 3(c)) develops as the extrusion-cycle increases, any distinct peak around 2.5° can not be found in XRD patterns from the C30A/oxaPS-hybrid (Figure 3(d)). Disappearance of characteristic XRD peak from C30A/oxaPS-hybrid indicates that most of silicate layers lose their crystallographic ordering in the hybrids. However, it is noteworthy that a broad peak around 6° develops as the extrusion-cycle increases. Appearance of broad peak around 6° is resulted from the fact that some intercalant molecules in bi-layer arrangement exude from the gallery, resulting in mono-layer arrangement of intercalated molecules between two adjacent silicate layers.[8] But the fraction of ordered silicate layers associated with the peak around 6° is thought to be small because the peak intensity is very weak.

Figure 4 shows the plots of peak area calculated by multiplying the peak height by full-width at half maximum as a function of extrusion-cycle. The peak area for C25A/oxaPS-hybrids increases with increasing extrusion-cycle, which means that the intercalation of oxaPS takes place slowly as the extrusion-cycle increases. However, the XRD peaks for C30A/oxaPS- and C30A/SAN-hybrids are much smaller than those for the C25A/oxa PS-hybrids. Thus it can be said that the crystallinities in the C30A/oxaPS- and C30A/SAN-hybrids decreased much more than those in the hybrids prepared using C25A. This might be resulted from the fact that the attractive interaction between intercalant and matrix polymer acts as the driving force to accelerate the intercalation of matrix polymer into the gallery of organophilic clays.

Figure 5 is a schematic diagram for the situation that a polymer chain intercalates into the gallery of silicate layers. It is expected that a large entropy loss takes place when a polymer chain in melt with a radius of gyration about several tens of
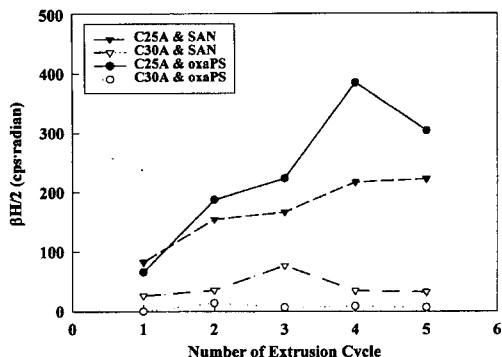
Figure 4. The plots of peak area calculated by multiplying the peak height (H, in count per second) by full-width at half maximum (β, in radian) as a function of extrusion-cycle.
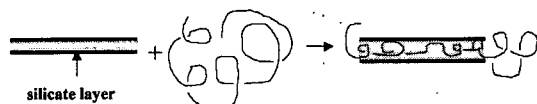

Figure 5. A schematic diagram for the situation that a polymer chain intercalates into the gallery of silicate layers. The shaded area indicates the intercalants between two adjacent silicate layers.

Figure 6. TEM micrographs of the (a) C25A/SAN-, (b) C30A/SAN-, (c) C25A/oxaPS-, and (d) C30A/oxaPS-hybrid.

nanometer intercalates into a narrow gallery of silicate layers with a thickness of about 1 nm. It is necessary that there is a strong interaction between polymer chain and the surface of silicate layer (and/or intercalant) in order for a long polymer chain to intercalate into a narrow gallery of silicate layers. Therefore the functional group in a polymer chain plays a crucial role in accelerating the intercalation of polymer chain with a smaller strength of interaction with the surface of silicate layer, such as polystyrene. Also, it is expected that the energetically favorable interaction between the functional groups in polymer chains and intercalants might accelerate the intercalation of polymer chain.

Figure 6 shows TEM micrographs for the various hybrids. It can be found that smaller nano-scale building blocks are distributed uniformly in the SAN hybrids (see Figure 6(a) and (b)), but any other evidence for truly exfoliated nanocomposite could not be found. More importantly, nano-scale building blocks in the C30A/SAN-hybrid are smaller than those in C25A/SAN-hybrid. This might be originated from the greater intercalation
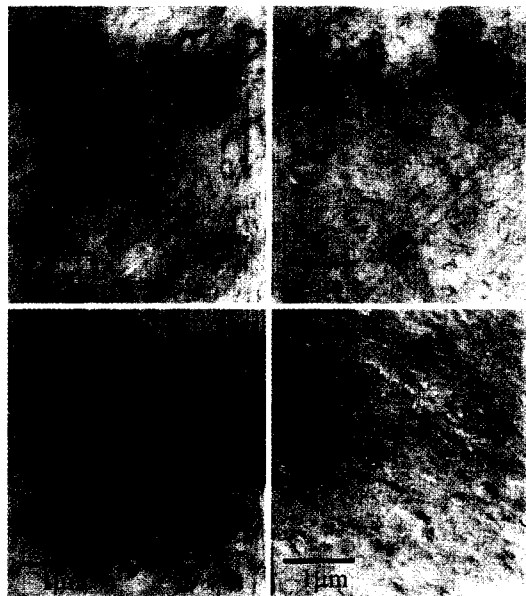
rate of SAN into the gallery of silicate layer of C30A than that of SAN into the gallery of silicate layer of C25A. The nano-scale building blocks are, also, found in the C25A/oxaPS-hybrid (Figure 6(c)). However, the nano-scale building blocks are not found in TEM micrograph of C30A/oxaPS-hybrid (Figure 6(d)). This indicates that most of silicate layers in the C30A/oxaPS-hybrid are exfoliated, and distributed in the sample (see Figure 7).

According to Balazs and his co-workers,[9,10] a truly exfoliated structure can only occur for a positive Flory-Huggins interaction parameter between polymer and clay layer, i.e. $\chi > 0$, though the polymers and silicate layers will ultimately demix. Also, they observed that an intercalated structure is expected when $\chi < 0$ from kinetic consideration. As the polymer diffuses through the energetically favorable gallery, it maximizes contact with the two confining layers. In effect, the polymer "glues" the two surfaces together as it moves through the interlayer. This "fused" condition could represent a kinetically trapped state and consequently, increasing the attraction between the polymer and clay sheets would only lead to intercalated,
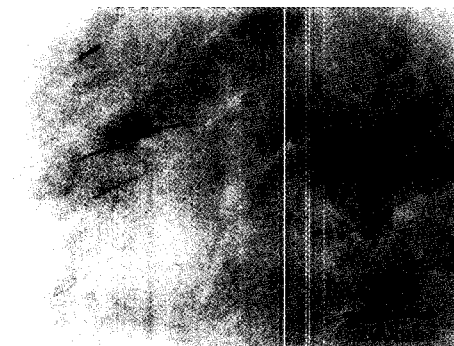
Korea Polym. J., Vol. 8, No. 3, 2000

123

Figure 7. TEM micrograph of the C30A/oxaPS-hybrid. The dark lines are 10-Å-thick silicate layers.

rather than exfoliated structures. The nitrile groups of SAN in the gallery between silicate layers might be complexed through hydrogen-bonding interaction with the hydroxyl groups on the surface of silicate layer of the clay. This prevents from retaining its coil-like conformation and gaining entropy of polymer chain in the gallery so that the adhesion force between two adjacent silicate layers is not reduced. However, the polymers containing lower content of functional group such as oxaPS can change its conformation easily to random coil in the gallery, so that the exfoliation of silicate layers can take place after the first extrusion. On the contrary, the intercalation of oxaPS in the C25A/oxaPS-hybrid takes place due only to the attractive force between the surface of silicate layer and the methylvinyloxazoline group of oxaPS. Thus the intercalation takes place more slowly than that in C30A/oxaPS-hybrid, resulting in no exfoliation of clay in the processing time used in this study, even though the matrix polymer has the ability to change its conformation to random-coil in the gallery of silicate layers. Thus a longer processing time might be needed to delaminate almost of silicate layers. Therefore the dispersion of silicate layers should be also explained by kinetic effects even though the exfoliation of clay is governed mainly by thermodynamic variables.

Conclusions

Clay-dispersed nanocomposites have been prepared by simple melt-mixing of two components, styrenic polymers and two different organophilic clays with a twin screw extruder. Dispersibility of silicate layers in clay-dispersed nanocomposite was studied by XRD- and TEM-analysis. It was found that if the interaction force between intercalant and matrix polymer is strongly attractive, the matrix polymer intercalates more rapidly into the gallery of silicate layers. Also, the intercalated polymer with lower content of functional group, i.e. oxaPS, leads to delaminate silicate layers of organophilic clay. The intercalated polymers with lower content of functional group are likely to change its conformation to gain entropy of polymer chain in the gallery, resulting in the exfoliation of silicate layers. However, the slower intercalation does not lead to the exfoliation of clay, even though the matrix polymer has the ability to change its conformation to random-coil in the gallery of silicate layers. Therefore the dispersion of silicate layers should be also explained by kinetic effects even though the exfoliation of clay is governed mainly by thermodynamic variables.

References

(1) M. S. Wang and T. J. Pinavaia, *Chem. Mater.*, **6**, 468 (1994).

(2) P. B. Massersmith and E. P. Giannelis, *Chem. Mater.*, **6**, 1719 (1994).

(3) T. Lan, P. D. Kaviratana, and T. J. Pinavaia, *Chem. Mater.*, **7**, 2144 (1995).

(4) S. D. Burnside and E. P. Gianellis, *Chem. Mater.*, **7**, 1597 (1995).

(5) R. A. Vaia, K. D. Jandt, E. J. Kramer, and E. P. Giannelis, *Macromolecules*, **28**, 8080 (1995).

(6) R. A. Vaia and E. P. Gianellis, *Macromolecules*, **30**, 7990 (1997).

(7) E. Hackett, E. Manias, and E. P. Gianellis, *J. Chem. Phys.*, **108**, 7410 (1998).

(8) J. T. Yoon, W. H. Jo, M. S. Lee, and M. B. Ko, *Polymer*, accepted.

(9) Y. Lyatskaya and A. C. Balazs, *Macromolecules*, **31**, 6676 (1998).

(10) A. C. Balazs, C. Singh, and E. Zhulina, *Macromolecules*, **31**, 8370 (1998).

124

Korea Polym. J., Vol. 8, No. 3, 2000